Modeling of Coherent Photoproduction in Hadronic Collisions I

GDR QCD Workshop on Coherence/Incoherence in Hadronic Diffractive Collisions at DIS and Hadron Colliders

M. B. Gay Ducati
Institute of physics, UFRGS, Brazil

Université Paris-Saclay, France

11-12/October/2023

Outlook

- Theoretical Framework
  - $\rightarrow$ The Exclusive Photoproduction.
  - $\rightarrow$ The Colour Dipole Models.
- Ultraperipheral Collisions (UPC)
  - $\rightarrow$ Rapidity Distributions
- Peripheral Collisions
  - $\rightarrow$ Rapidity Distribution
  - $\rightarrow$ Nuclear Modification Factor
  - $\rightarrow$ Centrality dependence
- New attempts $\rightarrow$ updates
  - $\rightarrow$ NLO
  - $\rightarrow$ FoCal

Hadronic Interactions

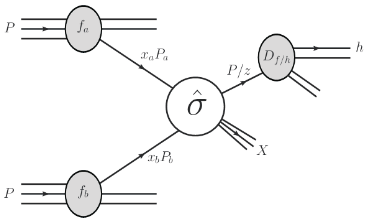

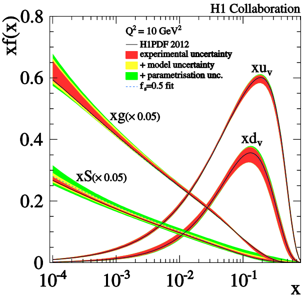

- The production cross section can be written as

$$\sigma_{hh\to hx} \propto f_{a/h}(x_1, Q^2) \otimes f_{b/h}(x_2, Q^2) \otimes \hat{\sigma}(ab \to cd) \otimes D_{h/c}(z_c, \hat{Q}^2)$$

$f_p(x, Q^2) \rightarrow$ Parton Distribution Functions (PDF's): MRST, GRV, CT18, MMHT14, ...

$\hat{\sigma}(ab \to cd) \rightarrow$ partonic subprocess $ab \to cd$: $q\bar{q} \to q\bar{q}$, $q\bar{q} \to gg$, $gg \to gg$, ...

$D_{h/c}(z_c, \hat{Q}^2) \rightarrow$ fragmentations functions of hadron h from a parton c.

Saturation Phenomena

- Some evolution equations:
- Linear equations
  - DGLAP
  - BFKL
- Non-Linear equations
  - AGL
  - JIMWLK
  - BK

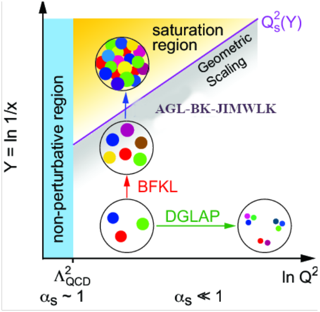

- At small-x, the gluon recombination process is important

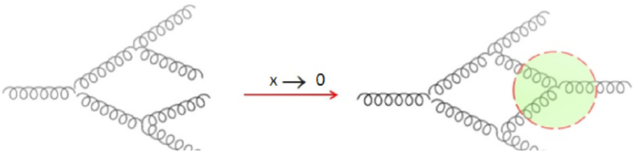

Balitsky-Kovchegov

The Balitsky-Kovchegov Equation

$$\partial_Y \langle T(x,z) \rangle = \frac{\bar{\alpha}}{2\pi} \int d^2z \mathscr{M}(x,y,z) [\langle T(x,z)\rangle + \langle T(z,y)\rangle - \langle T(x,y)\rangle - \langle T(x,z)\rangle \langle T(z,y)\rangle]$$

- This equation evolves $\langle T(x,y) \rangle$, average over all the dipole amplitudes $T(x,y)$.
- The evolution variable is the rapidity $Y \approx \ln 1/x$.
- $\bar{\alpha}_s = \alpha_s N_c/\pi$ and $\mathscr{M}(x,y,z) = \frac{(x-y)^2}{(x-z)^2(z-y)^2}$.
- The photon splitting in the $q\bar{q}$ pair with z and $1-z$ fraction of light cone momentum.
- The quark or antiquark can emit soft gluons ($z_2 \ll z_1$), which can also emit softer gluons.
- In the limit $N_c \to \infty$, these soft gluons can be considered as quark-antiquark pairs.

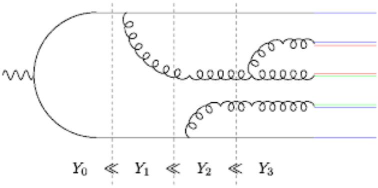

Colour Dipole Formalism

- Complementary information on gluons distribution can be obtained

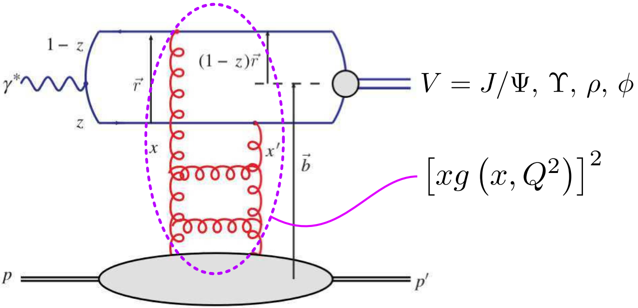

r is the dipole separation.
z(1-z) is the quark(antiquark) momentum fraction.
b is the dipole-target impact parameter.

Photo-Induced Interactions

- Diffractive production of vector mesons in hadron-hadron collisions.
- The process is characterized by large rapidity gaps in the final state.

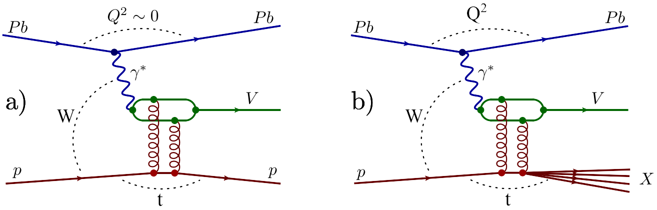

Coherent

$Q^2 \to$ photon virtuality.
$W^2 \to \gamma * p$ center of mass energy.
$t \to$ squared momentum transfer.

- We are interested in the first case: **Exclusive Photoproduction ($Q^2 \sim 0$),**

$$p \otimes Pb \to Pb \otimes V \otimes p$$

Weizsäcker-Williams Method

- Hadron-Hadron interaction $\rightarrow$ photon-hadron interaction

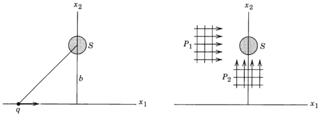

- Thus, the hadron process can be written in a simpler way

$$\sigma_X = \frac{dN(\omega)}{d\omega} \otimes {\sigma_X}^{\gamma}(\omega)$$

where the equivalent photon flux is written as [a]

$$\frac{dI(\omega)}{d\omega} = \frac{2q^2}{\pi}\left[\chi_{min}K_0(\chi_{min})K_1(\chi_{min}) - \frac{1}{2}\chi_{min}^2\left[K_1^2(\chi_{min}) - K_0^2(\chi_{min})\right]\right]$$

and σ_X^{γ} is the photoproduction cross section.

[a] UPC case, where $b > R_A + R_B$ and assuming the form factor F(q)=1, i.e, point-like charge.

The Photoproduction Cross Section

- For $\gamma - p$ interaction, the forward scattering amplitude is given by

$$\text{Im}\, A_{\text{proton}}(x, t=0) = \int\int \frac{d^2 r dz}{4\pi} \left(\psi_V^* \psi_\gamma\right)_T \sigma_{\text{dip}}^{\text{proton}}(x, r)$$

- $\left(\psi_V^* \psi_\gamma\right)_T$ - photon-meson wave function $\rightarrow$ Boosted Gaussian, better for the excited states;
  - $\sigma_{dip}^{proton}(x, r)$ - dipole cross section $\rightarrow$ GBW and CGC models.

- Then, the photoproduction cross section will be

$$\sigma\left(\gamma p \rightarrow Vp\right) = \frac{\left|\text{Im}\, A_{\text{proton}}(x, t=0)\right|^2}{16\pi B_V} \left(1 + \beta\left(\lambda_{eff}\right)^2\right) R_g^2(\lambda_{eff})$$

  - $x = \left(M_V^2 + Q^2\right) / \left(Q^2 + 2\omega\sqrt{s_{NN}}\right)$ and B_v is the slope parameter;
  - $\beta\left(\lambda_{eff}\right) = \frac{\text{Re}\, A_{proton}(x,t=0)}{\text{Im}\, A_{proton}(x,t=0)}$ restores the real contribution of the $A_{proton}(x, t=0)$;
  - $R_g^2(\lambda_{eff})$ - skewedness effect.

The Photoproduction Cross Section

- For $\gamma - A$ interaction, the forward scattering amplitude is given by

$$\mathrm{Im}\, A_{\rm nuc}(x, t = 0) = \int \int \frac{d^2 r dz}{4\pi} \left(\psi_V^* \psi_\gamma\right)_T \sigma_{\rm dip}^{\rm nuc}(x, r)$$

where

$$\sigma_{\rm dip}^{\rm nuc}(x, r) = 2 \int d^2 b' \left\{ 1 - \exp\left[-\frac{1}{2} T_A(b') \sigma_{\rm dip}^{\rm proton}(x, r) \right] \right\}$$

b' is the photon-nuclei impact parameter.

$T_A(b')$ is the nuclear profile function;

- Then, the photoproduction cross section will be

$$\sigma\left(\gamma A \to VA\right) = \frac{|\mathrm{Im}\, A_{nuc}(x, t=0)|^2}{16\pi} \left(1 + \beta\left(\lambda_{eff}\right)^2\right) R_g^2(\lambda_{eff}) \int_{t_{min}}^{\infty} |F(t)|^2\, dt$$

$F(t)$ - electromagnetic form factor and $t_{min} = \left(M_V^2 / 2\omega\gamma\right)^2$;

Dipole models

- The Golec-Biernat and Wüsthoff (GBW) model [1]:

- Model based on QCD-inspired phenomenology
  - The functional form of the dipole cross-section must have:

- For small r, $\sigma \propto r^2$ (Colour transparency);
- For large r, $\sigma \to constant$ (Ensures saturation).

$$\sigma_{q\bar{q}}^{GBW}(x,r) = \sigma_0[1 - \exp(-r^2 Q_s^2(x)/4)]$$

- $Q_s^2(x) = (x_0/x)^{\lambda_{GBW}}$ is the saturation scale;
- $\sigma_0 = 29.12$ mb, $x_0 = 0.41 \times 10^{-4}$, $\lambda_{GBW} = 0.29$ and $\chi^2/N_{dof} = 3.78$ - old fit -

for the extracted data from HERA with charm quark ($Q^2 \leq 10 GeV^2$ and $x \leq 10^{-2}$).

Re-evaluate for this fit[2]

- $\sigma_0 = 27.32$ mb, $x_0 = 0.42 \times 10^{-4}$,

$\lambda_{GBW} = 0.248$ and $\chi^2/N_{dof} = 1.60$.

[1] K. G. Biernat and M. Wüsthoff, Phys. Rev. D59, 014017 (1999); Phys. Rev. D60, 114023 (1999).

[2] K. G. Biernat and S. Sapeta, JHEP 1803 (2018) 102..

GFPAE

Dipole models

- The Iancu, Itakura and Munier (CGC) model [3]:

$$\sigma_{q\bar{q}}^{CGC}(x,r) = \sigma_0 \times \begin{cases} \mathcal{N}_0 \left(\frac{rQ_s}{2}\right)^{2(\gamma_s + (1/\kappa\lambda Y) ln(2/rQ_s))} & : rQ_s \leq 2 \\ 1 - e^{-A ln^2(BrQ_s)} & : rQ_s > 2 \end{cases}$$

  - $A = -\frac{\mathcal{N}_0^2 \gamma_0^2}{(1-\mathcal{N}_0)^2 ln(1-\mathcal{N}_0)}$ and $B = \frac{1}{2}(1-\mathcal{N}_0)^{-(1-\mathcal{N}_0)/(\mathcal{N}_0\gamma_s)}$.
- $Y = \ln(1/x)$, $\gamma_s = 0.73$, $\kappa = 9.9$ and $Q_s(x) = (x_0/x)^{\lambda/2}$.
- Free parameters: $\sigma_0 = 27.33$ mb, $\mathcal{N}_0 = 0.7$ and $\lambda = 0.22$.

Features:

For $r \ll 2/Q_s$ (small dipoles), $\mathcal{N}$ obtained from the saddle point approximation to the (LO) BFKL equation;

For $r \gg 2/Q_s$ (large dipoles), functional form of $\mathcal{N}$ obtained from solving the BK equation;

A and B restricted by continuity condition of $\mathcal{N}$ at $rQ_s = 2$

[3] **E. Iancu, K. Itakura, and S. Munier, Phys. Lett. B590, 199 (2004).**

Ultraperipheral Collisions

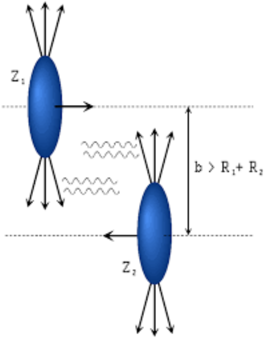

Results for $\sqrt{s} = 7$ TeV in pp collisions

- Comparison of the rapidity distribution for pp collisions with the LHCb data[4]

$$\frac{d\sigma}{dy}(pp \to p \otimes V \otimes p) = \omega \frac{dN_\gamma}{d\omega}\sigma(\gamma p \to Vp) + (y \to -y)$$

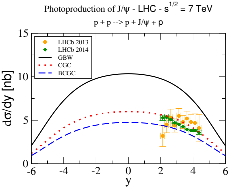

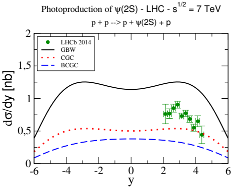

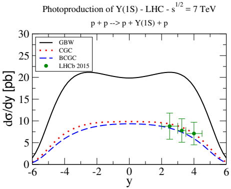

- *GBW* model overestimates the data.

Parametrization: M. Kozlov, A. Shoshi and W. Xiang - JHEP 0710 (2007) 020.

- The other models are consistent with the data of J/ψ and $Y(1S)$.

M. B. Gay Ducati, F. Kopp, M. V. T. Machado and S. Martins, PRD94, 094023 (2016).

4 **R. Aaij *et al.*, J. Phys. G40, 045001 (2013); J. Phys. G41, 055002 (2014); JHEP 1509, 084 (2015).**

GFPAE

Results for $\sqrt{s} = 7$ TeV in pp collisions

- Total cross section corrected by acceptance and branching ratio ($BR_{V\to\mu^+\mu^-}$).

$\sqrt{s} = 7$ TeV	GBW	CGC	b-CGC	LHCb
J/ψ [pb]	553.87	316.82	246.29	291±20 pb
$\psi(2S)$ [pb]	10.80	4.64	2.76	6.5±1.0 pb
$Y(1S)$ [pb]	22.05	9.25	8.05	9.0±2.7 pb
$Y(2S)$ [pb]	4.16	1.71	1.59	1.3±0.85 pb
$Y(3S)$ [pb]	2.07	0.87	0.83	<3.4 pb

Results for $\sqrt{s} = 5.02$ TeV in pA collisions

$$\frac{d\sigma}{dy}(pPb \rightarrow p \otimes V \otimes Pb) = \omega(y) N_\gamma^p(\omega(y)) \sigma_V^{\gamma Pb}(\omega(y)) + \omega(-y) N_\gamma^{Pb}(\omega(-y)) \sigma_V^{\gamma p}(\omega(-y))$$

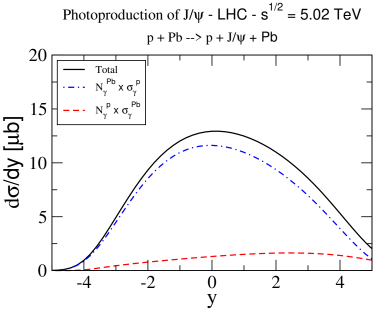

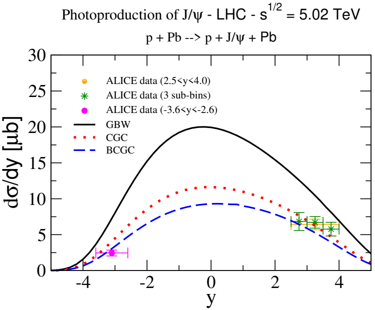

- Comparison of the rapidity distribution for pA collisions with the ALICE data (right plot)[5]

[5] B. B. Abelev et al. Phys. Rev. Lett. 113, (2014) 232504

Results for $\sqrt{s} = 5.02$ TeV in pA collisions

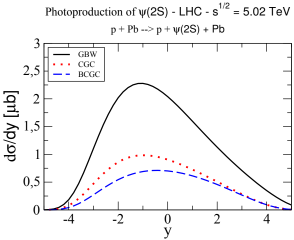

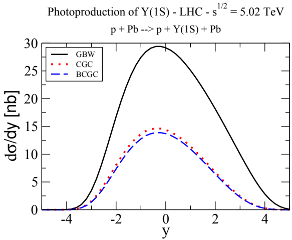

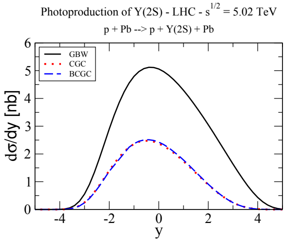

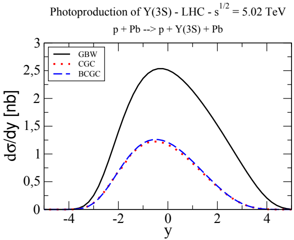

Results for $\sqrt{s} = 2.76$ TeV in AA collisions

- Comparison of the rapidity distribution for AA collisions with the ALICE data[6]

$$\frac{d\sigma}{dy}(AA \to A \otimes V \otimes A) = \omega \frac{dN(\omega)}{d\omega} \sigma(\gamma A \to VA) + (y \to -y)$$

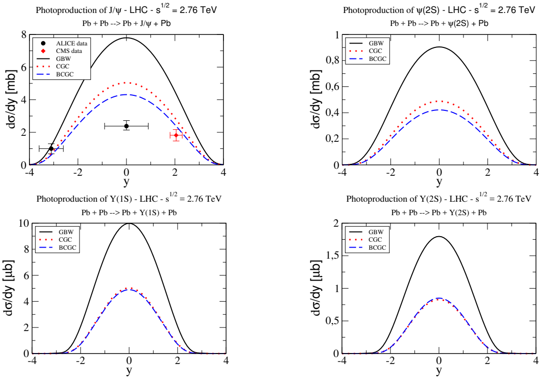

[6] B. Abelev *et al.*, Phys. Lett. B718, 1273 (2013); E. Abbas *et al.*, Eur. Phys. J. C73, 2617 (2013).

Peripheral Collisions

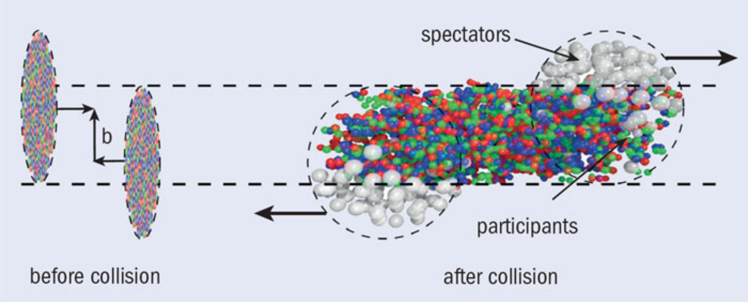

ALICE Measurements - J/ψ

Introduction

UPC Collisions

Peripheral Collisions

Experimental Data

b-Dependence

The eff. Photon Flux

The eff. Photonuclear Cross Section

Summary

- The nuclear modification factor (R_{AA}) is given by [7]

$$R_{AA}^{hJ/\psi} = \frac{N_{AA}^{J/\psi}}{BR_{J/\psi\to l^+l^-} \cdot N_{events} \cdot (A\times\varepsilon)_{AA}^{J/\psi} \cdot \langle T_{AA}\rangle \cdot \sigma_{pp}^{hJ/\psi}}$$

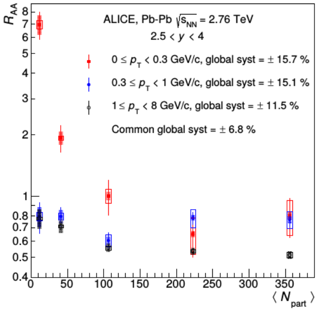

- $N_{AA}^{J/\psi} \to$ raw number of J/ψ
- $BR_{J/\psi\to l^+l^-} = 5.96\%$
- N_{events} [a] $\simeq 10.6\times 10^7$
- $(A\times\varepsilon)_{AA}^{J/\psi} \sim 11.31\%$
- $\langle T_{AA}\rangle$ [b] $= \begin{cases} 3.84\ \mathrm{mb}^{-1}, & 30\% - 50\% \\ 0.954\ \mathrm{mb}^{-1}, & 50\% - 70\% \\ 0.17\ \mathrm{mb}^{-1}, & 70\% - 90\% \end{cases}$
- $\sigma_{pp}^{hJ/\psi} = 0.0514\mu b$

[a] ALICE Coll., B. Abelev et al., PLB734, 314, (2014)

[b] ALICE Coll., B. Abelev et al., PRC88, 044909,

ALICE Measurements - J/ψ

- The Average Rapidity Distribution

$$\left.\frac{d\sigma}{dy}\right|_{2.5<y<4.0} = \frac{1}{\Delta y}\int_{2.5}^{4.0}\frac{d\sigma}{dy}dy$$

- ALICE measurements [8]

$p_T < 0.3$ GeV/c and $\sqrt{s_{NN}} = 2.76$ TeV

Cent.%	$N_{AA}^{J/\psi}$	$N_{AA}^{hJ/\psi}$	$N_{AA}^{\mathrm{excess}J/\psi}$	$d\sigma^{\mathrm{coh}}_{J/\psi}/dy$ [μb]
0-10	339±85±78	406±14±55	<251	<318
10-30	373±87±75	397±10±61	<237	<290
30-50	187±37±15	126±4±15	62±2±5	$73\pm44^{+26}_{-27}\pm10$
50-70	89±13±2	39±2±5	50±14±5	$58\pm16^{+8}_{-10}\pm8$
70-90	59±9±3	8±1±1	51±9±3	$59\pm11^{+7}_{-10}\pm8$

- $N_{AA}^{J/\psi}$ $\rightarrow$ raw number of J/ψ.
- $N_{AA}^{\mathrm{excess}J/\psi}$ $\rightarrow$ excess of J/ψ.
- $N_{AA}^{hJ/\psi}$ $\rightarrow$ raw hadronic number of J/ψ.

[8] ALICE Collaboration, J. Adam et al., Phys. Rev. Lett. 116, 222301, (2016)

STAR Measurements - J/ψ

- R_{AA} as a function of p_T for mid-rapidity ($|y| < 1$) [9].
- $\sqrt{s} = 200$ GeV for Au-Au and $\sqrt{s} = 193$ GeV for U-U.
- More intense excess for **60%-80%** centrality bin.
- The J/ψ excess is still present for **40%-60%** centrality class.

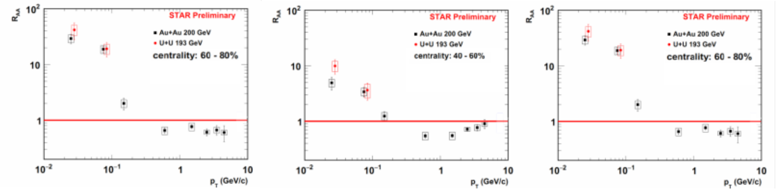

[9] W. Zha (STAR Collaboration), Journal of Physics: Conference Series 779, 012039 (2017).

b-Dependence Photon Flux

- For peripheral collisions → $N(\omega, b)$ with b-dependence [10],

$$\frac{dN(\omega,b)}{d\omega db^2} = \frac{Z^2\alpha_{qed}}{\pi^2\omega}\left|\int d^2k_T k_T^2 \frac{F(k)}{k^2} J_1(k_T b)\right|^2$$

- Yukawa potential+hard sphere (more realistic for lead) [11],

$$F(k) = \frac{4\pi\rho_0}{Ak^3}\left[\sin(kR_A) - kR_A\cos(kR_A)\right]\left[\frac{1}{1+a^2k^2}\right]$$

- $k^2 = (\omega/\gamma)^2 + k_\perp^2$.
- $\rho_0 = 0.1385$ fm and $a = 0.7$ fm
- A=208 and $R_A = 1.2A^{1/3}$ fm

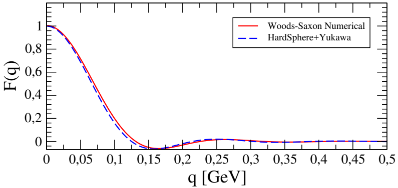

[10] F. Krauss, M. Greiner and G. Soff, Prog. Part. Nucl. Phys. 39, 503, (1997)

[11] K. T. R. Davies and J. R. Nix, Phys. Rev. C14, 1977 (1976).

Comparing the Form Factors

- Centrality classes and related impact parameters range:

Centrality Classes	Glauber Model		ALICE	
	b_{min} (fm)	b_{max} (fm)	b^{exp}_{min} (fm)	b^{exp}_{max} (fm)
30%-50%	7.77	10	8.55	11.04
50%-70%	10	11.87	11.04	13.05
70%-90%	11.87	13.47	13.05	14.96

- Analysis of the different form factors

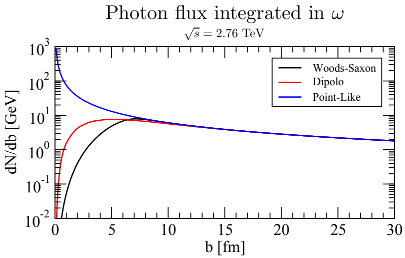

Point Like (used in UPC)

- $F(k^2) = 1$.

Dipole Form Factor

- $F_{dip}(k^2) = \frac{\Lambda^2}{\Lambda^2 + k^2}$.

Woods-Saxon+Yukawa

- $F_{WSY}(k^2) = \frac{4\pi\rho_0}{Ak^3}\left[\sin(kR_{Pb}) - kR_{Pb}\cos(kR_{Pb})\right]\left[\frac{1}{1+a^2k^2}\right]$.

GFPAE

The Effective Photon Flux

- Considering an effective photon flux [12]

$$\sigma_X = \int \omega \frac{dN^{eff}(\omega)}{d\omega} \sigma_X(\omega)$$

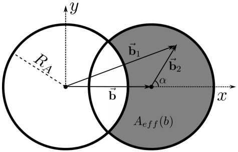

- **Hypothesis:** Only spectators interact coherently with the photon.

- In this scenario, $\frac{dN^{eff}(\omega,b)}{d\omega}$ can be described as [13]

$$N^{eff}(\omega,b) = \frac{1}{A_{eff}(b)} \int N^{usual}(\omega,b_1)\theta(b_1 - R_A)\theta(R_A - b_2)d^2b_2$$

- $A_{eff} = R_A^2\left[\pi - 2\cos^{-1}(b/2R_A)\right] + (b/2)\sqrt{4R_A^2 - b^2}$ and $b_1^2 = b^2 + b_2^2 + 2bb_2\cos(\alpha)$

[12] M. K. Gawenda and A. Szczurek, Phys. Rev. C93, 044912, (2016).

[13] M. B. Gay Ducati and S. Martins, Phys. Rev. D97, 116013, (2018).

The Effective Photonuclear Cross Section

- The forward scattering amplitude is given by

$$\mathrm{Im}\, \mathscr{A}_{nuc}(x,t=0) = \int \frac{d^2r dz}{4\pi} \left(\psi_V^* \psi_\gamma\right)_T \sigma_{\mathrm{dip}}^{\mathrm{nucleus}}(x,r)$$

where

$$\sigma_{\mathrm{dip}}^{\mathrm{nucleus}}(x,r) = 2\int d^2b' \left\{1 - \exp\left[-\frac{1}{2} T_A(b')\sigma_{\mathrm{dip}}^{\mathrm{proton}}(x,r)\right]\right\}$$

- Consistency with the construction of $N^{eff}(\omega,b)$, restrict $\sigma_{dip}^{nucleus}(x,r)$:

$$\sigma_{\mathrm{dip}}^{\mathrm{nucleus}}(x,r) = 2\int d^2b_2 \Theta(b_1 - R_A)\left\{1 - \exp\left[-\frac{1}{2} T_A(b_2)\sigma_{\mathrm{dip}}^{\mathrm{proton}}(x,r)\right]\right\}$$

  - $b_1^2 = b^2 + b_2^2 + 2bb_2\cos(\alpha)$.

GFPAE

Our results for dσ/dy

- Essentially, three modification were considered

  - b-dependence ($S1$).
  - Effective photon flux ($S2$).
  - Effective Photonuclear cross section ($S3$) .

The scenario S3 uses the effective photon flux and the effective photonuclear cross section.

- Comparing with ALICE data (S3),

Average Rapidity Distribution: $2.5 < y < 4.0$

GBW / CGC	$d\sigma^{\rm theo}_{J/\psi}/dy$ [μb]	$d\sigma^{\rm exp}_{J/\psi}/dy$ [μb]
30%-50%	73 / 61	$73 \pm 44^{+26}_{-27} \pm 10$
50%-70%	78 / 66	$58 \pm 16^{+8}_{-10} \pm 8$
70%-90%	75 / 63	$59 \pm 11^{+7}_{-10} \pm 8$

- Better agreement for CGC model considering 50% $\rightarrow$ 90%.

Our results for R_{AA}

- Black circles (S1): only the b-dependence
  - Best agrees with the data only in the more peripheral region;
- Green losangle (S2): b-dependence + effective photon flux
  - Better results were achieved for the more central classes;
- Blue triangle (S3): All the three modifications was applyed
  - A slight correction in direction to data in relation to last case;

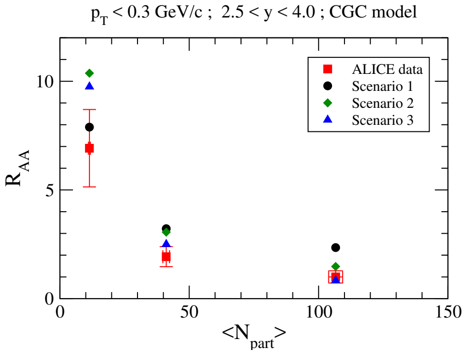

Our results: Quark Matter 2022

J/ψ photoproduction in peripheral collisions

- **Transition from ultra-peripheral to peripheral collisions:**
  - Need to account for the geometrical constraints of a given impact parameter
  - Modification of the photon flux / photonuclear cross section

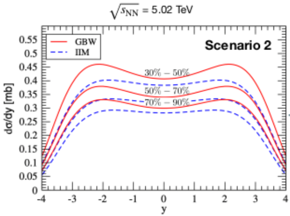

Scenario 1: UPC like
Scenario 2: effective photon flux
Scenario 3: effective photon flux + photonuclear cross section

IIM: Color Glass Condensate approach
GBW: light cone dipole formalism

M. B. Gay Ducati et al., PRD 97 (2018) 11

7

Quark Matter 2022 - A. Neagu

Our results: Quark Matter 2022

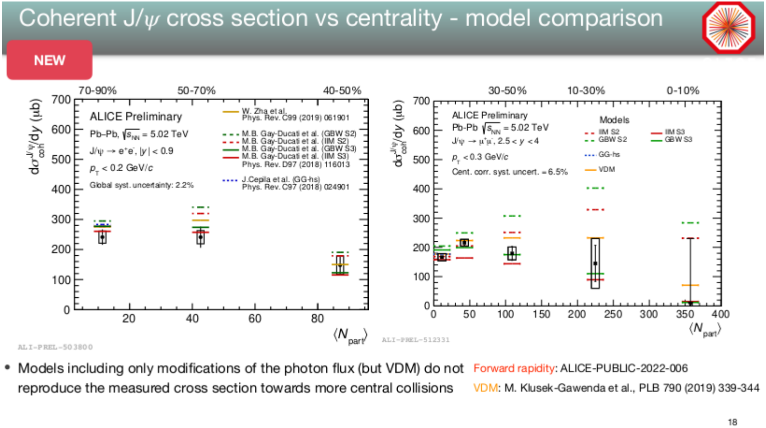

Quark Matter 2022 - A. Neagu

Our results: Quark Matter 2022

Coherent J/ψ cross section at forward rapidity

NEW

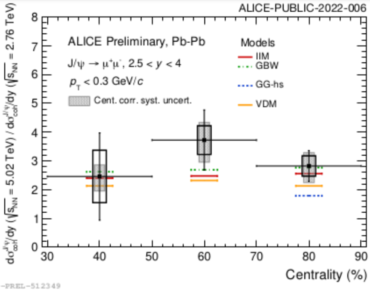

- Ratio of the measurements at $\sqrt{s_{NN}}$ = 5.02 TeV and $\sqrt{s_{NN}}$ = 2.76 TeV shows no centrality dependence within uncertainties
- Fair agreement of the measured ratio to models (except GG-hs) within uncertainties

19

Quark Matter 2022 - A. Neagu

Our results: Quark Matter 2023

Coherent J/ψ photoproduction in Pb–Pb collisions: centrality dependence

ALICE

- **Both measurements at mid and forward rapidity don't show a significant centrality dependence***
- Measurements are qualitatively described by a large number of models developed for UPC and extended to account for the nuclear overlap

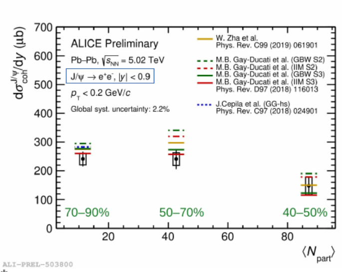

arXiv:2204.10684

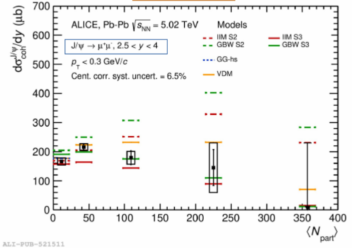

70–90% 50–70% 30–50% 10–30% 0–10%

* The cross section is not normalized to the centrality interval width

A. Shatat, QM, Sept. (3-9) 2023

6

Quark Matter 2023 - A. Shatat

GFPAE

Our results: Quark Matter 2023

y-dependence of the coherent J/ψ photoproduction cross section

ALICE

- A strong rapidity dependence is seen
- Models initially developed for VM photoproduction in UPC and modified for PC **are able to describe qualitatively the magnitude of the cross section, but fail at reproducing the *y*-dependence, similarly to UPC**. NEW

Models considerations:

GG-hs: photon flux with constraints on impact parameter range

Zha : assumptions on photon-pomeron coupling (nucleus+spectator)

GBW S3, IIM S3 } effective photon flux and photonuclear cross section considered w.r.t UPC calculations (see next slide)

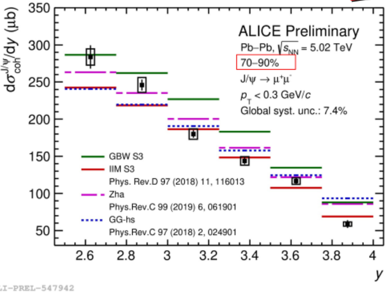

A. Shatat, QM, Sept. (3-9) 2023 12

Quark Matter 2023 - A. Shatat

GFPAE

Introduction

UPC Collisions

Peripheral Collisions

Experimental Data

b-Dependence

The eff. Photon Flux

The eff. Photonuclear Cross Section

Summary

NLO study in pQCD

- Scale dependence
- Gluons and quarks contributions (!)
- Nuclear effects

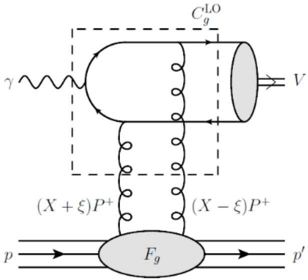

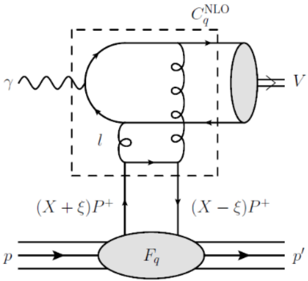

- only gluons GPD's

- Gluons + quarks GPD's

[Ivanov et al., Eur. Phys. J. C 34 (2004) no. 3, 297]

How about data (LHC)?

Figures from C. Flett, PhD thesis [Flett:2021xsl]

NLO study in pQCD: amplitude

K. Eskola et al., arXiv:2203.11613 [hep-ph]

$$\mathcal{M}^{\gamma N \to VN} \propto \langle O_1 \rangle_V^{1/2} \int_{-1}^{1} dx [T_g(x,\xi) F^g(x,\xi,t) + T_q(x,\xi) F^{q,S}(x,\xi,t)],$$

- $\langle O_1 \rangle_V^{1/2}$ NRQCD element
- T_g *and* T_q hard scattering functions from pQCD[1], scale dependent (μ_F, μ_R)
- F^g *and* $F^{q,S}$ GPDs[2], nonperturbative (μ_F)

$$|\mathcal{M}|^2 = |\mathcal{M}_G^{\text{LO}} + \mathcal{M}_G^{\text{NLO}}|^2 + |\mathcal{M}_Q^{\text{NLO}}|^2 + 2\Big[\text{Re}(\mathcal{M}_G^{\text{LO}} + \mathcal{M}_G^{\text{NLO}})\text{Re}(\mathcal{M}_Q^{\text{NLO}}) + \text{Im}(\mathcal{M}_G^{\text{LO}} + \mathcal{M}_G^{\text{NLO}})\text{Im}(\mathcal{M}_Q^{\text{NLO}})\Big].$$

[1] D. Y. Ivanov, A. Schafer, L. Szymanowski, G. Krasnikov, Eur. Phys. J. C 34 (2004) no. 3, 297 [Erratum: Eur.Phys.J.C 75, 75 (2015)]

Comparison of LO for exclusive J/ψ photoproduction in PbPb

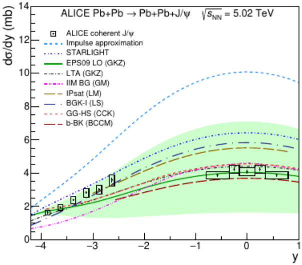

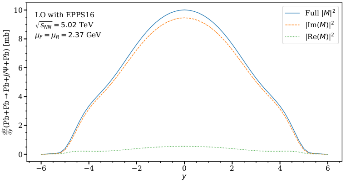

- In pQCD and QCD models
- Linear and non-linear evolution equations.
- The data favour those models

featuring moderate nuclear shadowing.

S. Ragoni, on behalf of the ALICE Collaboration, arXiv:2305.03616v1

- In pQCD
- The $|Re(M)|^2$ in LO is almost irrelevant.

K. Eskola et al., arXiv:2203.11613 [hep-ph]

NLO for exclusive J/ψ photoproduction in PbPb (pQCD): contributions of quark, gluons and interference term

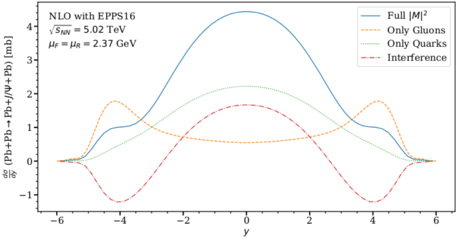

- How the quark, gluons and interference terms contribute to final amplitude.

K. Eskola et al., arXiv:2203.11613

NLO for exclusive J/ψ photoproduction in PbPb (pQCD)

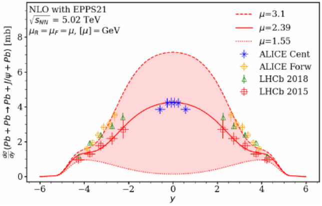

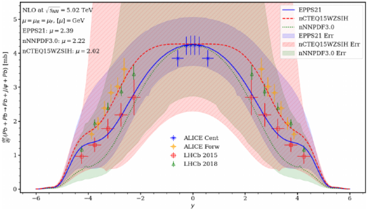

- New LHCb forward data agrees with ALICE data also at forward direction. Sensible to μ choice.

- However, large uncertainties remain due to the nuclear PDFs. A comparison between EPPS21, nNNPDF3.0 and nCTEQ15WZSIH uncertainties is shown.

K. Eskola et al., arXiv:2303.12630v1 [hep-ph]

NLO for exclusive J/ψ photoproduction in PbPb (pQCD) vs colour dipole picture LO (UPC)

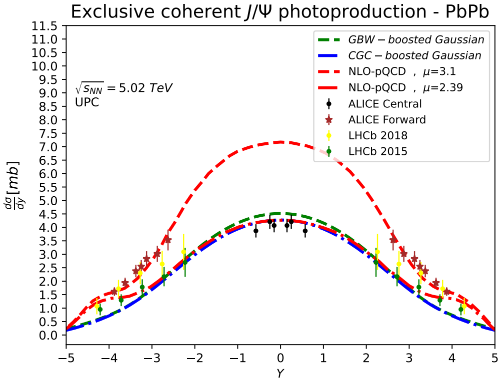

- The data does not support any particular model.
- Our results with dipole picture in LO are shown by the blue solid line and the green dashed line.

K. Eskola et al., arXiv:2203.11613 (pQCD)

Energy dependence for J/ψ photoproduction within colour dipole picture: NLO

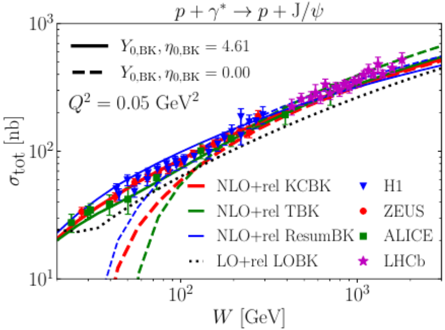

Relativistic correction proportional to the heavy quark velocity squared v^2

and next-to-leading order to longitudinal vector meson.

- The smallest possible evolution rapidity Y_0,BK = 0 (or η_0,BK = 0 in the case of TBK evolution).

H. Mäntysaari et al. JHEP 08 (2022) 247

Energy dependence for J/ψ photoproduction: CGC, NLO BFKL and others

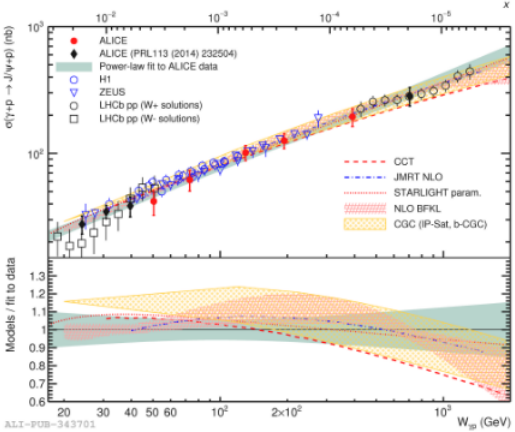

- These models consider only gluons: NLO BFKL (K-factor), JMNRT NLO (K-factor).

|t|-dependence of coherent and incoherent J/ψ photonuclear production

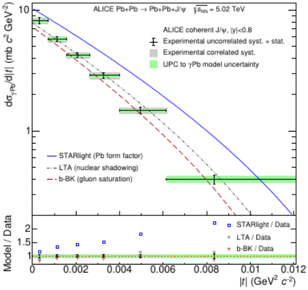

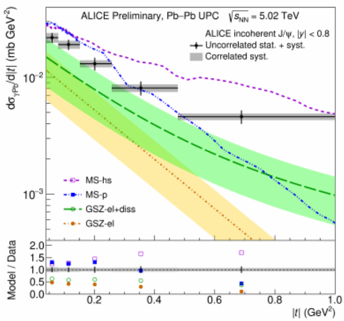

- Coherent J/ψ is sensitive to the average of spatial distribution of the gluons.

- Incoherent J/ψ is sensitive to the gluons variance.

None of the models manages to describe both the slope and the normalization of the data distribution.

- It is a powerful observable to measure gluon saturation.

S. Ragoni, on behalf of the ALICE Collaboration, arXiv:2305.03616v1

FoCAL (forward electromagnetic and hadronic calorimeter)

FoCal (Forward Electromagnetic and Hadronic Calorimeter)

FoCal calorimeter consist of two calorimeters, an electromagnetic calorimeter (FoCal-E) and an hadronic calorimeter (FoCal-H), intended to be installed in the ALICE experiment in 2026.

The FoCal-E will be a sampling calorimeter made of tungsten and silicon.

The FoCal-H will be a sampling calorimeter "spaghetti" model made of lead and scintillating fibers.

With FoCal, it will be possible to study the J/Ψ mesons through their decay into e^+e^- pairs, which can be detected by the calorimeter through the production of electromagnetic showers.

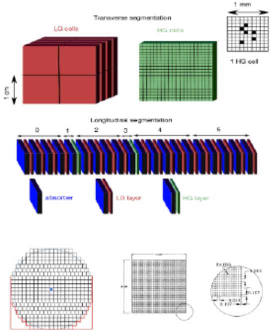

- Simulation using STARlight to generate J/ψ and ψ' events. Where the data is grouped into superclusters and matched with the physical primary particles;
- Expected yields result in a clear separation between the resonances.

Conclusions

- Exclusive quarkonium photoproduction off protons in p-Pb UPC
  - Probe the gluon density at low x
  - Search for gluon saturation effects
- Light vector mesons photoproduction in UPC provides
  - Test theoretical models
  - Study shadowing effects in the nonperturbative regime
- Photoproduction in peripheral collisions
  - Complements the knowledge on hadroproduction
  - Improve analytical description on centrality dependence
- LO calculations require comparison to NLO
  - Role of quark contribution in heavy vector meson production
  - Confrontation data on different energies, y’s, pt’s, centralities...

And a Look Ahead...

- UPC Pb-Pb collisions for exclusive coherent J/ψ, the current data cannot distinguish between NLO pQCD and LO dipole models;

- J/ψ photoproduction within NLO dipole picture requires the relativistic correction v^2 as well as longintudinal vector meson function at NLO to describe the data;

- Study dipole colour models with DGLAP evolution equations for peripheral collisions;

- FoCal is the best suited LHC detector subsystem to exploit this energy; it will probe the gluon densities of protons and heavy ions down to Bjorken-x values below 10^{-6}.